Research Article

Sources, distribution and bioavailability of sedimentary phosphorus species in coastal areas off Changjiang Estuary

Pei Sun Loh[1] · Xing-Rui Huang[1] · Chen-Yu Ying[1] · Jianxiong Hu[1] · Zhang-Hua Lou[1] · Xue-Gang Chen[1] · Shuangyan He[1] · Zong-Pei Jiang[1] · Ai-Min Jin[1]

Received: 13 April 2020 / Accepted: 16 June 2020 / Published online: 24 June 2020

Abstract
The Changjiang Estuary (CE), two transects along the Andong salt marsh (AD-A and AD-C) south-west of Hangzhou Bay, and three salt marshes on Zhoushan Island (ZS-A, ZS-B and ZS-C) were coastal zones receiving different flow regimes and human activities. In this study, sedimentary P species consisting of exchangeable P (Ex-P), iron P (Fe-P), authigenic P, detrital P (De-P) and organic P (OP) were determined in these sediments. The objectives of this study were to evaluate the degree of P pollution and the potential for these sediments to release P into the environment. Authigenic P was the largest fraction in AD-A, AD-C, CE, ZS-A and ZS-B (42–62%), followed by Ex-P (28–33%), Fe-P (4–19%), OP (2–8%) and De-P (1–2%); except in ZS-C where Ex-P was the most abundant (57.86%), followed by authigenic P (24.45%), Fe-P (12.34%), OP (2.85%) and De-P (2.49%). High portions of authigenic P indicate presence of apatite minerals; low levels of OP and De-P suggest low P pollution and low contribution from riverine input. The sedimentary total P (TP) in these locations (ranged from 91.30 to 324.74 mg/kg) indicates the risk of P pollution was very low. However, the bioavailable P (Ex-P, Fe-P and OP) constituted approximately 37–73% of TP. Thus, these locations are prone to release P from Ex-P fraction under oxic conditions and from Fe-P fraction under anoxic conditions.

Keywords Salt marsh · Estuary · Sediment · **P**hosphorus species · Bioavailable phosphorus

1 Introduction

Coastal zones such as salt marshes are important carbon and nutrient sink [1, 2], and regulator of nutrient and pollutants [3–5]. These coastal zones are affected by extreme weather conditions and climate change phenomenon such as sea level rise which threaten to submerge marsh plants [6–8]. They are affected by human activities such as embankment [9], land conversion [10], pollution [11, 12] and the presence of reservoirs reducing sediment input for marsh accretion [13]. Phosphorus (P) pollution is common in coastal areas such as estuaries [14, 15] and salt marshes [4, 16]. Nutrient pollution can have detrimental effect on plants and animals, and eventually human health, due to environmental degradation and effect on food source [17]. In some cases, problems related to P pollution persist although P input from external sources has been reduced. This is due to internal sedimentary P loading, a phenomenon which has been well studied in lake ecosystems [18, 19]. Internal P loading has also resulted in release of bioavailable P to the water column and causing increased primary production in coastal environments [20]. Only certain P species can be released to the water and become bioavailable [21], hence, the importance of determination of sedimentary P species.

Authigenic P fraction includes biogenic apatite such as fish bones and teeth, P combined with $CaCO_3$ and authigenic carbonate fluorapatite. This P species precipitates in pore water and contributes to P burial in sediments; thus, this is the most stable P form and it is non-bioavailable.

✉ Pei Sun Loh, psloh@zju.edu.cn; ✉ Ai-Min Jin, aiminjin@163.com | [1]Ocean College, Zhejiang University, Zhoushan 316021, China.

Authigenic P represents materials from erosion processes and can serve as a tracer of organic matter sources. Exchangeable-P (Ex-P) is loosely bound and represents the most labile P fraction. Sources of Ex-P include dissolved P from runoff and P adsorbed on eroded sediments. Ex-P is formed when organic matter decomposition releases phosphate ions which are then adsorbed onto clay minerals and the surfaces of Fe oxides and hydroxides, making them the main carriers of Ex-P in the sediment. Ex-P can be released to overlying water during resuspension of fine particles or changes in pH, temperature, water dynamics, redox condition and during organic matter decomposition. The iron-bound-P (Fe-P) fraction is pH and redox sensitive, and a source of internal P loading during anoxic conditions when P is released from sediments due to reduction and dissolution of P from iron oxyhydroxides to iron (II) compounds. Detrital-P (De-P) is derived from magma or igneous or metamorphic rocks, or from riverine inputs of terrestrial materials. Organic P (OP) is related to discharge from domestic sewage and agriculture effluents and is released as phosphate during the aerobic decomposition of organic matter [9, 22–24].

Sequential phosphorus (P) extraction methods have been used to elucidate the different P forms in these sediments, such as loosely bound or exchangeable P (Ex-P), Fe-P, authigenic P, De-P, OP and inorganic P (IP). Determination of sedimentary P species has been used to study P released to water environments and P bioavailability in lakes [22, 23, 25] and rivers [26, 27]. Many studies of different sedimentary P forms have also been carried out in marine environments, such as surface and core sediments in the Gulf of Gdansk [28], surface sediments in the Gulf of Mexico [20], sediment cores from the Arabian Sea oxygen minimum zone [29], surface sediments in the central Pacific Ocean [30] and sediment cores from the sulphidic black sea [31]. Along the coastal zones of China, studies of sedimentary P species include investigation of sediment cores from the Quanzhou Bay estuary [32], surface and core sediments from the eastern coast of Hainan Island in the South China Sea [24], surface [33] and core sediments [34] from the East China Sea, and sediment cores from the Yangtze River Estuary [35] and Jiazhou Bay [36]. Nearer to our study areas, the sedimentary P species along the Changjiang Estuary and East China Sea have been studied [33–35], but the locations in these studies are farther to the sea in comparison with the locations in the current study. Besides, few studies have determined the sedimentary P species in salt marshes, for example, the Min River Estuary marsh [37]. Thus, this study provided a good opportunity to determine the sedimentary P species in salt marshes in this region.

In this study, surface sediments from the Andong salt marsh at the south-west of Hangzhou Bay, three salt marshes along Zhoushan Island (two salt marshes at the south and another at the north of the island) and a transect across the Changjiang Estuary were subjected to sequential P extraction to evaluate the levels of Ex-P, Fe-P, authigenic P, De-P and OP. The objectives of this study were to investigate the degree of P pollution in these coastal environments, and to determine whether the P in these systems could be released into the environment and become otherwise bioavailable. Our study areas include various locations receiving different flow regimes and human activities. Besides, estuaries are submerged by water, whereas salt marshes are intermittently submerged. Hopefully, comparison between these different coastal systems will provide a good opportunity to improve understanding on the P dynamics in these systems.

2 Materials and methods

2.1 Study areas

The major locations in this study were, namely the Changjiang Estuary, the salt marsh at the south-west of Hangzhou Bay and the salt marsh along the north-east and south of Zhoushan main island. Changjiang Estuary is a funnel-shaped estuary which is discharged by the Changjiang River, the largest river in China [38]. Hangzhou Bay is located south of Changjiang Estuary and is discharged by the Qiantang and Cao-E Rivers, but receives most of its materials from the Changjiang River [39]. As materials from the Changjiang River enters Hangzhou Bay through the north side of the bay and leave through the south side of the bay [38, 39], the input from the Changjiang River most probably affect Hangzhou Bay as well as the salt marsh at the south-west of the bay [40]. Zhoushan archipelago is situated at the outlet of Hangzhou Bay. Zhoushan Island has experienced about 50% expansion of urban areas from 1995 to 2011 due to enhancement of socioeconomic activities [35], and this expansion has affected the coastal zone [41]. As a result of the relative decline of contribution from the Changjiang River, the effect due to contributions from the Qiantang River, as well as relict and rock materials from Zhoushan Island, has increased, especially along the southern coast of the main Zhoushan island [42]. Hence, it will be interesting to compare the sedimentary P species among these study areas which receive different flow regimes and human activities.

2.2 Sampling

The Andong salt marsh is a micro-tidal salt marsh with an area of 300 km^2 and located at the south-western edge of Hangzhou Bay. The sampling locations in the Andong salt

marsh were two transects of about 2 km spanning from the landward to the coastal side of the marsh. There were eight locations along Transect A and eight sampling locations along Transect C. Andong salt marsh samples were obtained by scooping of the surface sediments into plastic bags. There were six sampling locations spanning from the Changjiang Estuary, numbered from the river mouth to farther offshore as "20", "4", "6", "11", "13" and "21". The sediments along the Changjiang Estuary were collected using a grab sampler. The sediments from the salt marsh and estuary were transported back to the laboratory in cooler.

Three different salt marshes from the main Zhoushan island were sampled, two located at the south side of the island and one smaller salt marsh surrounded by a small bay at the north-east side. In comparison with the Andong salt marsh, the Zhoushan salt marshes are smaller, with lengths of about 2–3 km and widths of about 500 m. The salt marsh situated in the north-east is the smallest of the three. They were sampled parallel to the coast; surface sediments were scooped into plastic bags. These were transported straight to the laboratory and without preservation in cooler due to the colder sampling time.

The Changjiang Estuary and Andong salt marsh samples were collected in 2014; the Zhoushan sediments were collected in 2018. Sampling locations and timetable were presented in Yuan et al. [40], "Appendix 1" and Fig. 1. The sampling dates and locations details of the Zhoushan salt marshes are presented in "Appendix 2" and in Fig. 1. All sampled sediments were immediately transported to the laboratory. In the laboratory, sediments were dried at 45 °C for a few days and homogenized using a mortar and pestle.

2.3 Sequential P extraction

Sequential P extraction procedures were carried out using the method described by Ruttenberg [43]. For the first P fraction, 0.5 g of dry sediment was weighed into a 50-mL

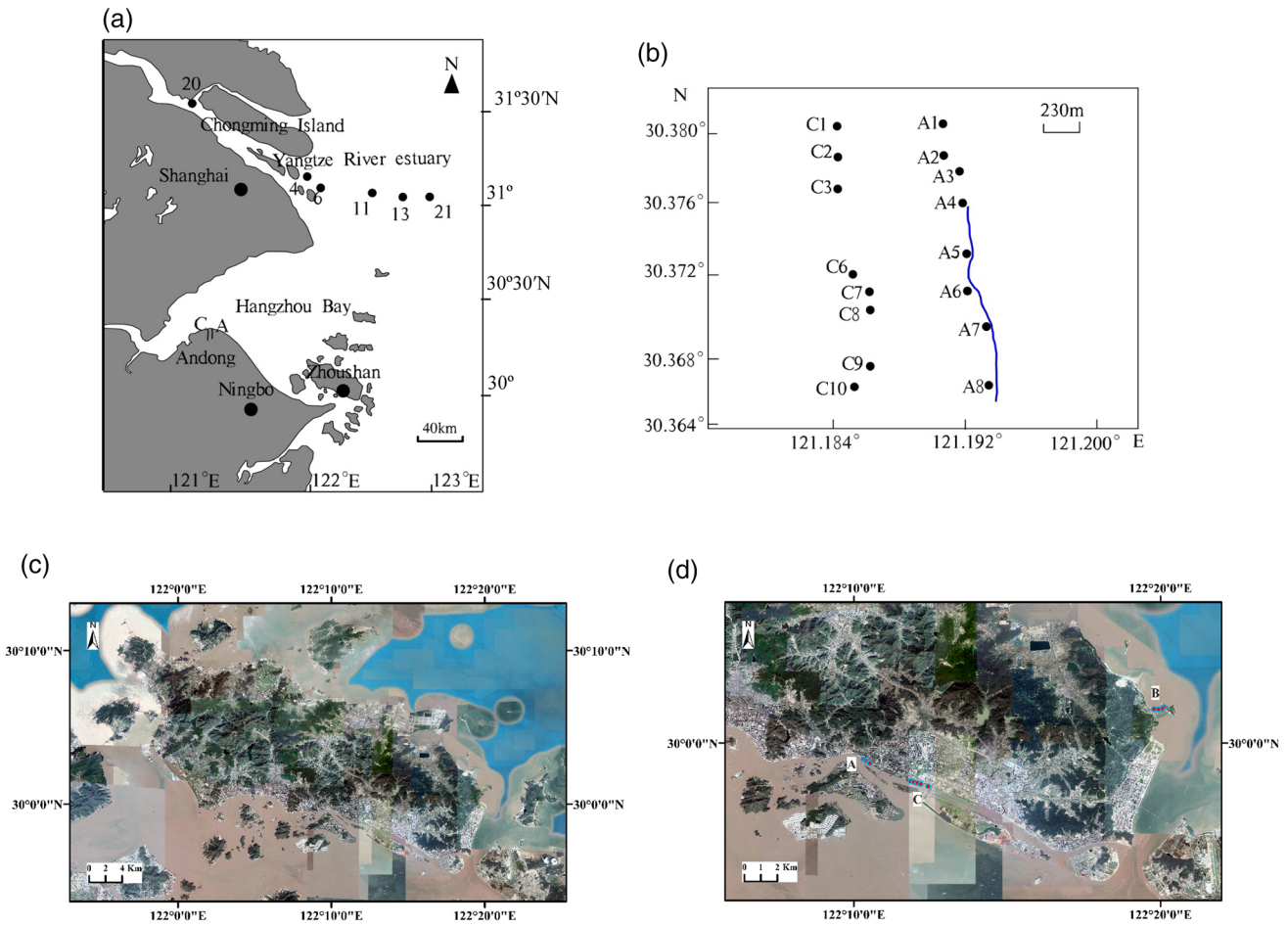

Fig. 1 Maps showing **a** the sampling locations along the Changjiang Estuary, Andong salt marsh and Zhoushan, **b** locations along the Andong salt marsh magnified, **c** the main Zhoushan Island, **d** the locations of the three sampling locations A, B and C; and individual sampling locations in **e** B, **f** A and **g** C

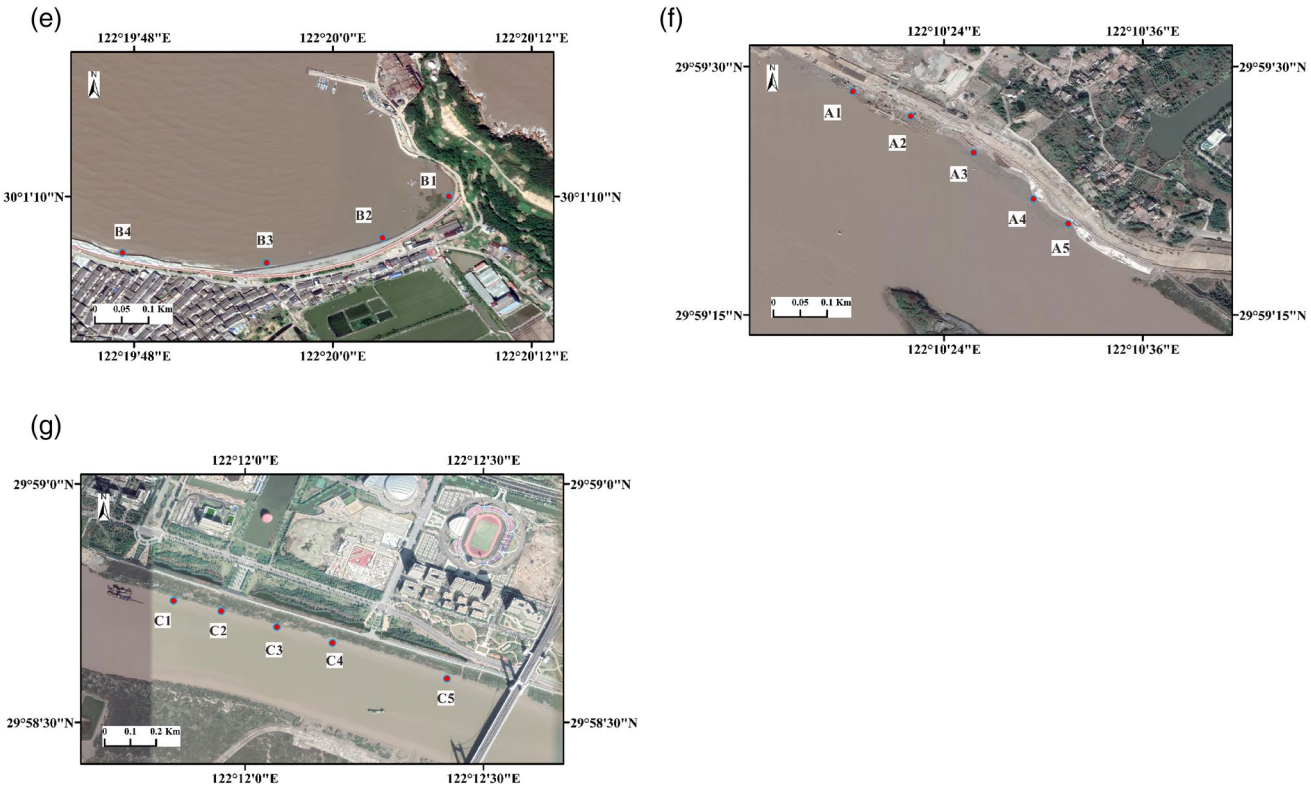

Fig. 1 (continued)

centrifuge tube, 20 mL of $MgCl_2$ was added, and the solution was adjusted to pH 8 with Na_4OH. P was extracted by shaking for 2 h at room temperature (RT), after which the content was centrifuged, and the supernatant was decanted and set aside. Another 20 mL $MgCl_2$ was added to the residue, and the process was repeated. The residue was washed with 10 mL H_2O for 2 h, centrifuged, and then, the supernatant was removed and saved. The supernatants from this step were saved to evaluate their Ex-P content. For the second fraction, 20 mL of citrate–dithionite–bicarbonate (CDB) solution was added to the residue from the first. Extraction was carried out by shaking for 8 h at RT. This content was then centrifuged, and the supernatant decanted and saved. Then, 20 mL $MgCl_2$ was added to the residue and shaken for 2 h, followed again by centrifugation and extraction of the supernatant. Subsequently, the residue was washed with 10 mL H_2O for 2 h, centrifuged, and then, the supernatant was removed and saved. The supernatant from this fraction was set aside to evaluate its Fe-P content. Next, 20 mL of pH 4 acetate buffer was added to the remaining residue and shaken for 6 h at RT, after which the mixture was centrifuged, and the supernatant was saved. The residue was then washed twice with $MgCl_2$, centrifuged again, and the supernatant was removed and set aside. The residue was finally washed with 10 mL H_2O, centrifuged one more time, and the supernatant was again removed and saved. The supernatants from this step were set aside to evaluate its authigenic P content. In the next step, 1 M HCl was added to the residue and shaken for 16 h, after which the content was centrifuged, and the supernatant was saved to be analysed for De-P. Finally, the residue was moved to a crucible and dried in an oven at 80 °C for one day, followed by combustion at 550 °C for 5 h. The residue was cooled, and 1 M HCl was added and shaken for 16 h. The extraction procedures are also shown in Fig. 2.

The supernatant from this step was set aside to evaluate for OP. Inorganic P (IP) was the sum of Ex-P, Fe-P, authigenic P and De-P. Total P (TP) was the sum of IP and OP. All P concentrations were determined colorimetrically with molybdenum blue complex and absorbance measurements at 885 nm wavelength using a UV-8000 UV–visible spectrophotometer (METASH, Shanghai, China).

3 Results

Detailed results of sedimentary P forms from the Changjiang Estuary (CE), Andong salt marsh transects A and C (AD-A and C) and Zhoushan salt marshes A, B and C (ZS-A, B and C) are presented in "Appendix 3". The ranges, means and percentages of each P form are presented in Table 1.

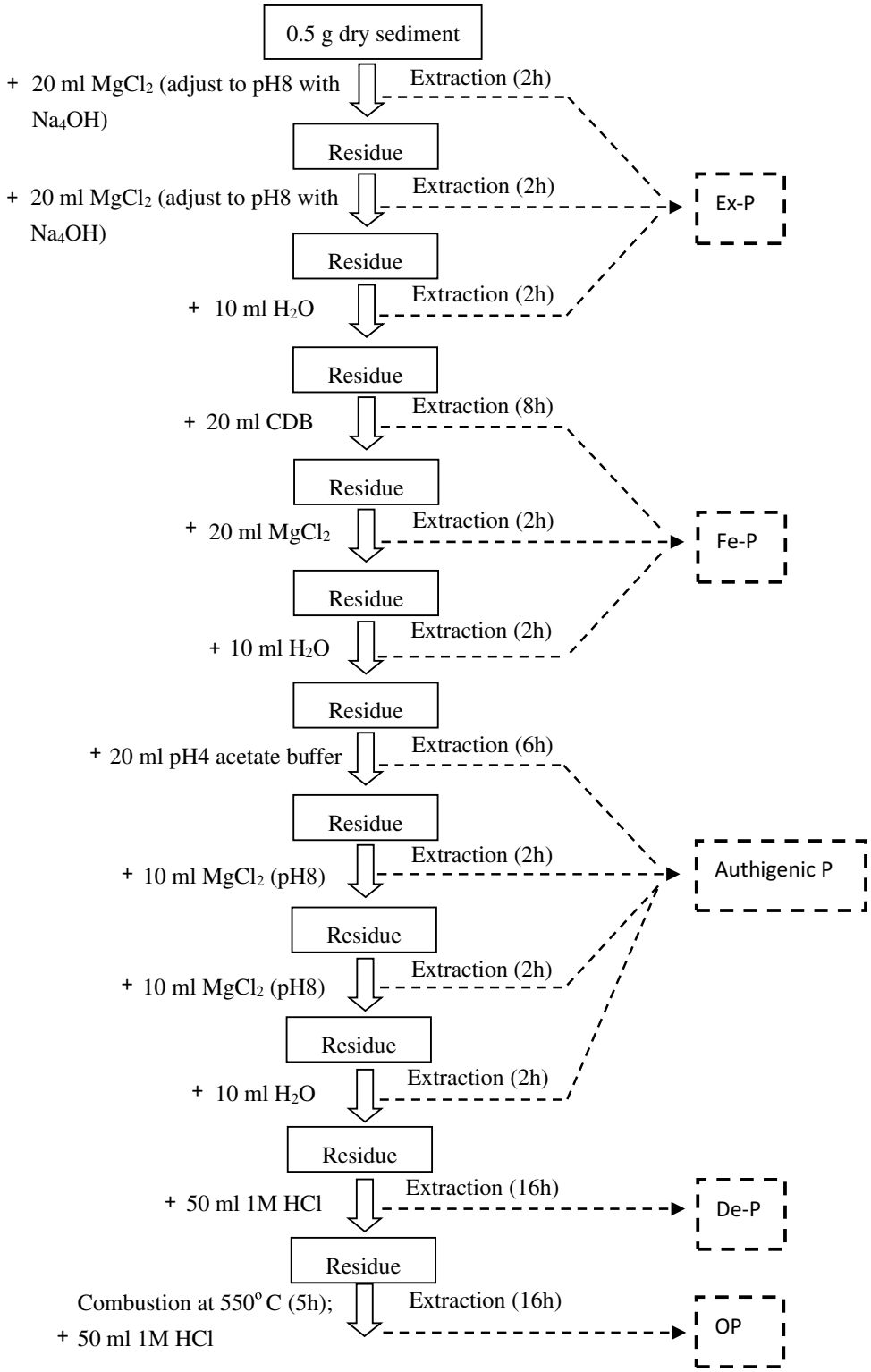

Fig. 2 Flow diagram of the sequential extraction procedures (following Ruttenberg, 1992)

3.1 Comparison of sedimentary P forms in CE, AD and ZS

The order of contribution from each sedimentary P form is shown in "Appendix 4" and Fig. 3. Authigenic P was the highest P fraction in all but one of the study areas. Authigenic P composed of around 41–45% of TP for AD-A and -C and CE, and more than 60% TP in ZS-A and -B salt marshes. Ex-P was the second highest P species, representing around 28–33% TP in these areas. Only ZS-C has Ex-P

SN Applied Sciences (2020) 2:1280 | https://doi.org/10.1007/s42452-020-3090-8

Table 1 Ranges, averages and percentages of sedimentary P forms

Loc	Concentration ranges and averages in terms of mg/kg and % (in brackets)							
	Ex-P	Fe-P	Authigenic P	De-P	OP	IP	BAP	TP
AD-A	20.68–49.94 Ave = 36.26 (29.01%)	12.46–40.13 Ave = 24.86 (19.22%)	37.98–89.58 Ave = 54.93 (42.81%)	1.98–3.56 Ave = 2.63 (2.10%)	4.45–11.98 Ave = 8.70 (6.86%)	86.67–149.00 Ave = 118.68 (93.14%)	46.30–85.43 Ave = 69.83 (55.09%)	91.30–159.47 Ave = 127.38
AD-C	41.38–71.43 Ave = 53.43 (33.77%)	16.72–50.60 Ave = 27.35 (16.85%)	45.23–91.54 Ave = 67.00 (41.77%)	1.95–3.78 Ave = 2.83 (1.79%)	7.36–13.47 Ave = 9.24 (5.83%)	125.06–188.41 Ave = 150.61 (94.17%)	65.54–104.62 Ave = 90.02 (56.44%)	132.50–196.99 Ave = 159.86
CE	33.38–60.13 Ave = 46.59 (30.64%)	9.20–31.19 Ave = 21.04 (13.78%)	59.61–83.05 Ave = 68.39 (45.67%)	2.14–2.97 Ave = 2.58 (1.74%)	3.05–18.55 Ave = 12.53 (8.16%)	118.50–176.82 Ave = 138.60 (91.84%)	52.37–106.11 Ave = 80.16 (52.59%)	121.55–191.61 Ave = 151.13
ZS-A	82.05–106.30 Ave = 91.24 (31.16%)	5.36–26.08 Ave = 12.88 (4.45%)	155.60–224.62 Ave = 180.11 (61.25%)	2.38–3.54 Ave = 2.99 (1.02%)	1.86–16.00 Ave = 6.09 (2.12%)	268.39–322.85 Ave = 287.22 (97.88%)	92.17–123.83 Ave = 110.21 (37.73%)	270.37–324.74 Ave = 293.31
ZS-B	63.61–94.29 Ave = 80.56 (28.49%)	13.39–21.73 Ave = 17.40 (6.12%)	157.13–196.17 Ave = 175.67 (61.97%)	2.37–4.27 Ave = 3.08 (1.08%)	1.00–9.87 Ave = 6.54 (2.34%)	250.93–306.02 Ave = 276.71 (97.66%)	95.21–119.24 Ave = 104.50 (36.95%)	256.48–307.02 Ave = 283.25
ZS-C	63.31–116.09 Ave = 88.51 (57.86%)	9.50–32.46 Ave = 19.11 (12.34%)	16.90–65.07 Ave = 37.91 (24.45%)	2.38–5.04 Ave = 3.88 (2.49%)	2.15–10.24 Ave = 4.59 (2.85%)	121.33–163.85 Ave = 149.40 (97.15%)	87.21–129.19 Ave = 112.20 (73.06%)	123.78–172.58 Ave = 153.99

Ex-P = exchangeable P; Fe-P = iron-bound P; De-P = detrital P; OP = organic P; IP = inorganic P; BAP = bioavailable P; TP = total P; IP = Ex-P + Fe-P + authigenic P + De-P; TP = OP + IP; BAP = Ex-P + Fe-P + OP

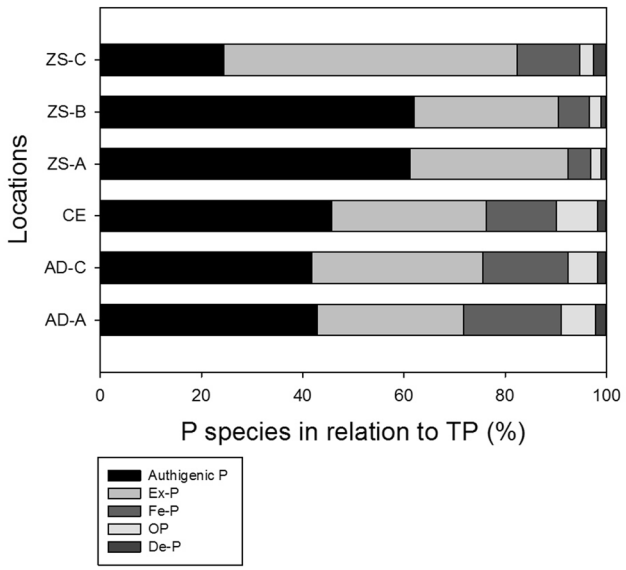

Fig. 3 Percentages of P species in relation to TP

as the largest P fraction, at an average of 57.86% of TP, followed by authigenic P, at 24.45% of TP. Fe-P was between 12 and 19% TP in AD-A and -C, CE and ZS-C, and only 4–6% TP in ZS-A and -B (Fig. 2).

Bioavailable P was the sum of Ex-P, Fe-P and OP [21]. The bioavailable P percentages of TP for the study areas were as follows: ZS-C (73.06%) > AD-C (56.44%) > AD-A (55.09%) > CE (52.59%) > ZS-A (37.73%) > ZS-B (36.95%). Bioavailable P was the highest in ZS-C, making up around 73.6% of TP, mainly due to the high concentration of Ex-P therein. The Andong salt marsh and Changjiang Estuary each had around 55% bioavailable P, and ZS-A and -B had around 37% bioavailable P.

3.2 Spatial variations of sedimentary P species

The spatial distributions of sedimentary P species are shown in Fig. 4. The sediments along two transects of the Andong salt marsh showed a slight decrease of Ex-P and noticeable decrease in OP from the land towards the coastal zone. De-P decreased towards the coast in AD-A but increased towards the coast in AD-C. Fe-P and authigenic P were both slightly higher at locations near the coast. TP and IP decreased overall towards the coast for transect AD-A but increased slightly towards the coast along transect AD-C. Along the Changjiang Estuary, TP, IP, authigenic P, Ex-P and Fe-P increased towards location 11 but decreased further offshore. Ex-P, authigenic P and IP were the lowest at the furthest distance from shore, whereas Fe-P and OP were the highest. Zhoushan A and C salt marshes spanning from west to east were divided into locations Al to A5 and C1 to C5, respectively. Ex-P, Fe-P, De-P and OP decreased from A1 towards A5, and Ex-P, Fe-P and OP increased from C1 towards C5. Both authigenic P and IP showed the opposite trends of the other P forms, increasing from A1 to A5, and decreasing from C1 to C5. All locations of ZS-B were parallel to the landwards side of a 500-m-wide salt marsh and showed intermittent high and low concentrations of the different P species.

4 Discussion

4.1 Sources of sedimentary P species

Our results showed that authigenic P made up the largest portion of P species in the AD and CE salt marshes (contributing around 40% of TP) and the ZS-A and -B (around 60% of TP). Authigenic P was positively correlated with IP in AD and CE, and with TP in ZS-A and B ($p < 0.05$; "Appendix 5"), indicating the importance of contribution of this P fraction to IP and TP. Both Ex-P and OP were negatively correlated to authigenic P. Ex-P could be released from the sediments due to physical disturbances, and OP could be released from the sediments from organic matter decomposition. The P released from these fractions could then be used in the formation of authigenic P. However, most of the areas in this study have low OP, suggesting that the authigenic P was mostly derived from the Ex-P fraction.

Higher Fe-P fractions in AD-A, AD-C, CE and ZS-C (at between 12 and 19% of TP) suggest that these locations were oxic and the sediments showed an affinity for Fe and P adsorption. Higher Fe-P also means that these locations can release much P under anoxic conditions. Conversely, the lower Fe-P in ZS-A and ZS-B could indicate that these locations were anoxic and have released a certain amount of Fe-P into the environment. The OP fraction made up about 6% of TP in the AD salt marsh, about 8% of TP in the CE and about 2% of TP in Zhoushan salt marshes, suggesting that these areas received relatively less P pollution from sewage and agricultural waste. De-P made up around 1% of TP across all study areas, indicating very little P derived from riverine terrestrial organic matter.

Bioavailable P was the highest portion of TP at ZS-C, representing around 73.06% of TP, due to the highest abundance of Ex-P and Fe-P here. The AD salt marsh and CE each had about 55% bioavailable P, also from Ex-P and Fe-P. ZS-A and B had about 37% bioavailable P, contributing less P to their local environments than ZS-C. Of all study areas, AD, CE and ZS-C are the most likely to release P from their Ex-P fractions following organic matter decomposition and Fe-P fractions under anoxic conditions. Hence, even though authigenic P was the largest fraction in these study areas, these sediments are still

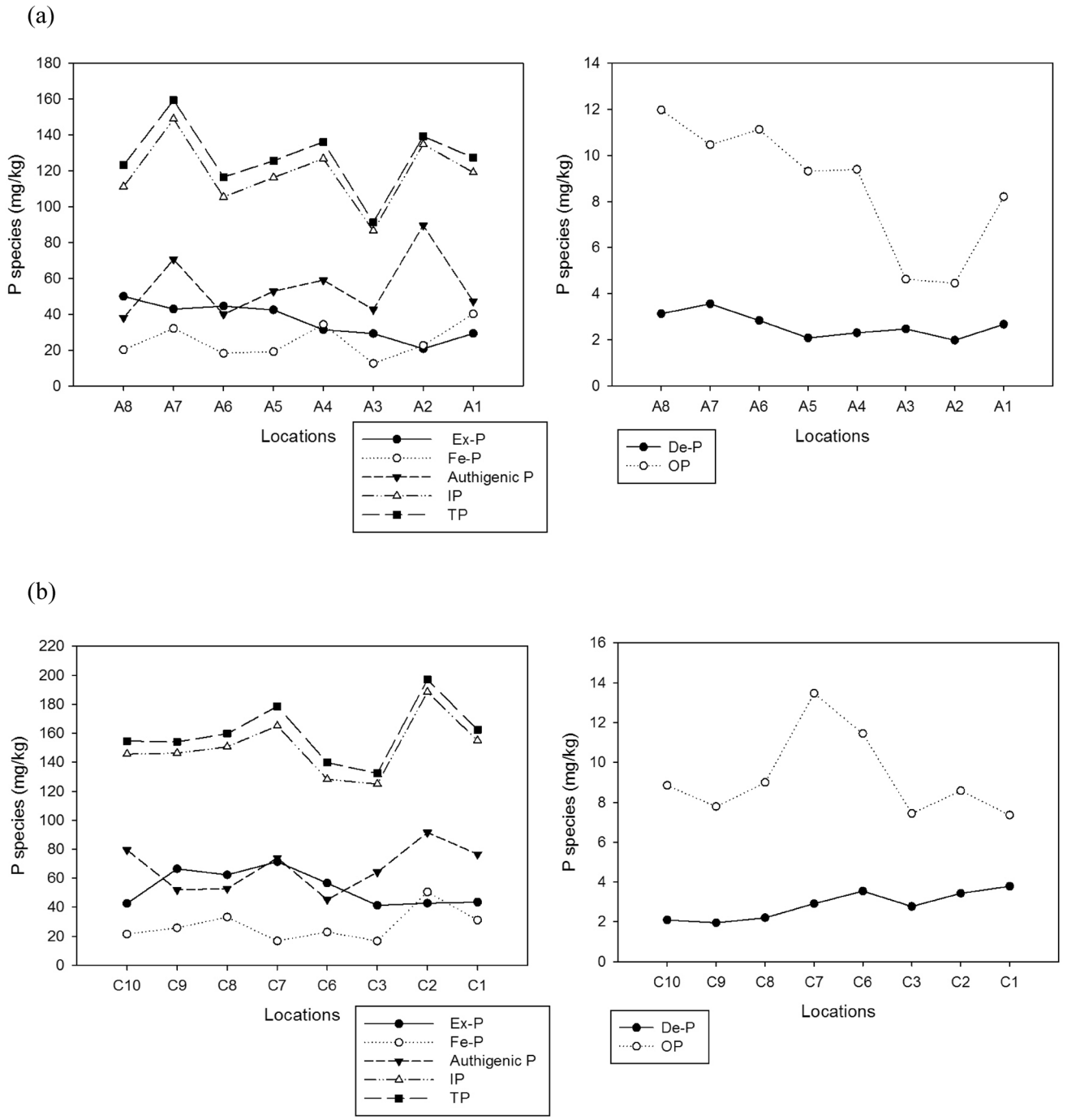

Fig. 4 Sedimentary P species along **a** Andong salt marsh Transect A (AD-A), **b** Andong salt marsh Transect C (AD-C), **c** Changjiang Estuary (CE) and **d** Zhoushan salt marshes A and C (ZS-A and ZS-B)

prone to release P into the environments as they were composed of about 50% or more bioavailable P.

4.2 Distribution of sedimentary P species

Along the AD salt marsh, OP and Fe-P levels decreased from the locations nearest the land towards those near the coast. This could be due to smaller particle sizes near land that increased farther towards the coast. Significant correlations among particle size and Fe-P, Ex-P, and authigenic P have been observed in the Bay of Seine and the Loire and Gironde Estuaries [44], and loosely bound-P was found adsorbed onto fine particles in Lakes Volvi and Korona [45]. Another potential explanation for the decrease

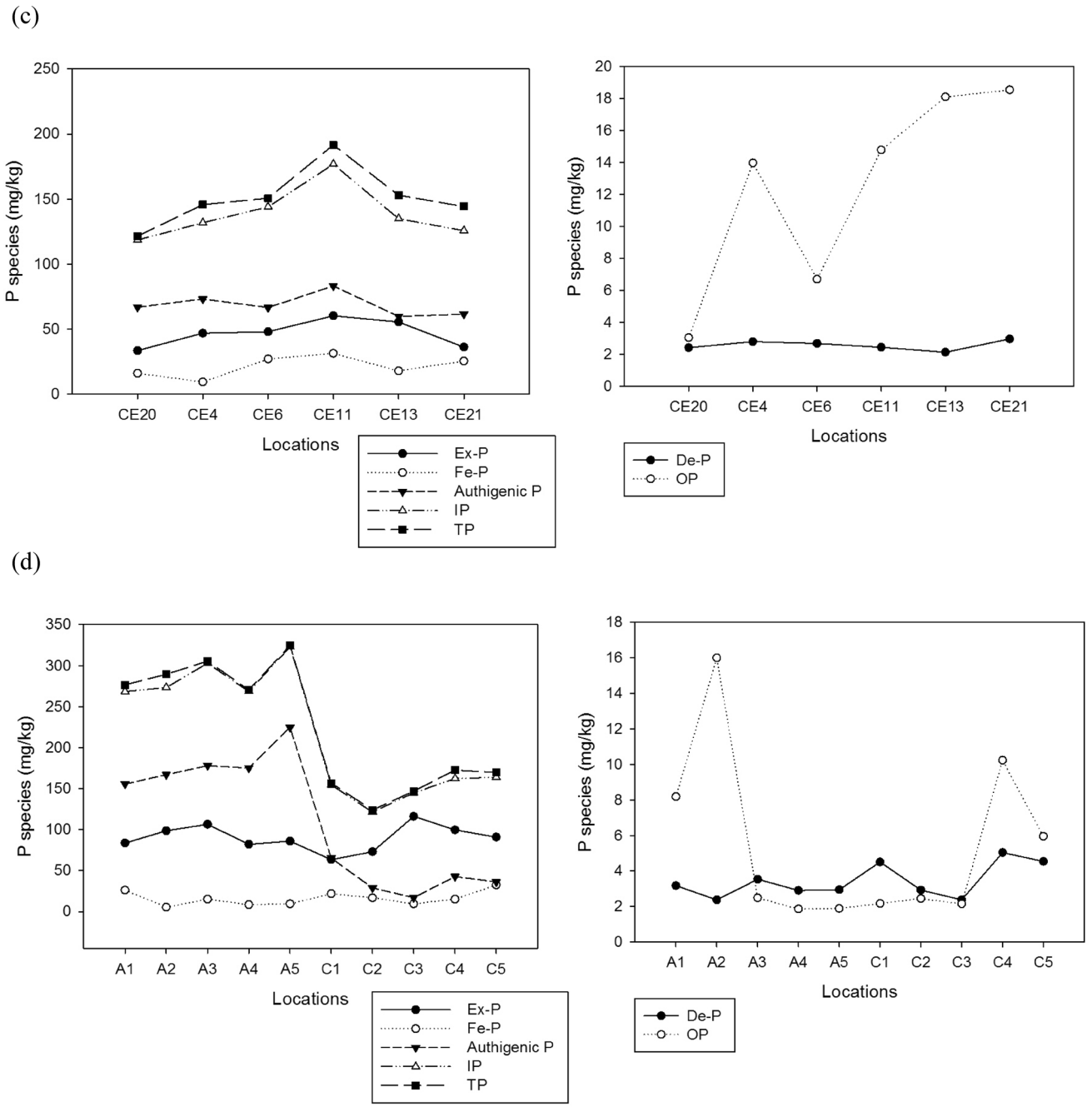

Fig. 4 (continued)

in OP and Ex-P farther away from the coast could be continuous organic matter decomposition during transport of materials farther offshore, resulting in continuous release of P. This P might then have adsorbed onto Fe oxides and hydroxides and carbonate fluorapatite, as indicated by the slightly higher Fe-P and authigenic P proportions observed farther offshore.

Meng et al. [46] found that fine-grained particles predominated in the Changjiang large-river delta-front estuary and along the Zhe-Min coastal areas, whereas the Changjiang River mouth and outer shelf region off the muddy area contained coarser, sandy materials. Lower TOC and OP contents were found at the river mouth and outer shelf region associated with more sandy materials, and higher TOC contents were found in the muddy areas. However, the De-P fraction showed the opposite trend, likely due to the contribution of eroded soils from the upper river basins. Besides, these are enriched with

Table 2 Study areas and their sedimentary TP

Locations	Surface sediment or core	Total P (mg/kg)	References
Zhoushan A, B and C	Surface sediment	293.31, 283.25, 153.99	This study
Andong A and C	Surface sediment	127.38, 159.86	This study
Changjiang Estuary	Surface sediment	151.13	This study
East China Sea (ECS)	Sediment core	369.83–739.97	[35]
Changjiang Estuary and adjacent East China Sea	Surface sediment	465–663.4	[42]
East China Sea	Sediment core	416.5–638.5	[43]
East of Hainan Island	Surface sediment and core	246.76–692.54	[33]
Sishili Bay, China	Sediment core	466.24–669.29	[44]
Central Pacific Ocean	Surface sediment	409.2–3689	[31]
Caspian Sea	Surface sediment	431–594	[45]

Table 3 Order of sedimentary P species in different locations

Locations	Order of sedimentary P species	References
AD-A,C; CE; ZS-A,B	Authigenic P > Ex-P > Fe-P > OP > De-P	This study
ZS-C	Ex-P > Authigenic P > Fe-P > OP > De-P	This study
Gulf of Mexico	Authigenic P > De-P > Fe-P > OP > Ex-P	[29]
Pacific Ocean	Authigenic P > De-P > OP > Fe-P > Ex-P	[31]
East China Sea	De-P > OP > Fe-P > Authigenic P	[35, 42]
East China Sea	De-P > Authigenic P > OP > Fe-P	[34]

Ca-P and De-P composed of minerals such as quartz and feldspar, which a have a higher affinity for larger particles [46]. Our results along the CE showed an overall increasing trend of OP as the distance from the shore increased, probably due to increased adsorption by smaller particles. The trends of Ex-P, Fe-P and authigenic P showed an increase, followed by a decrease in the two last locations. The overall increasing trends of P species from the river mouth to mid-location could be due to increased accumulation and increased adsorption with smaller particles, followed by a decrease in the contents of these P fractions farther offshore, possibly due to dilution with marine materials.

The sampling locations in the Zhoushan salt marsh A and C regions spanned from west to east from A1 to A5 and C1 to C5. Ex-P, Fe-P, De-P and OP decreased from A1 to A5 and increased from C1 to C5. This trend seems to be due to an overall materials flow from the west to east, resulting in increased accumulation of these materials, including P, at C5. However, trends for Ca-P diverged from the other P forms, indicating that this P species might be from localized source, perhaps at locations along ZS-A where construction was being carried out on a walkway and embankment along the landward side of the marsh.

4.3 Comparisons with sedimentary P species from other locations

The average concentration of TP in the surface sediments in the areas evaluated in this study was as follows: ZS-A (293.31 mg/kg) > ZS-B (283.25 mg/kg) > AD-C (159.86 mg/kg) > ZS-C (153.99 mg/kg) > CE (151.13 mg/kg) > AD-A (127.38 mg/kg). These values were lower than in other locations, such as East China Sea sediment cores [47], Changjiang Estuary and adjacent East China Sea surface sediments [46], northern Gulf of Mexico sediment cores [20], central Pacific Ocean surface sediments [30], Sishili Bay, China [48], the eastern coast of Hainan Island surface sediment [24], East China Sea core sediments [34] and Caspian Sea surface sediments [49] (Table 2).

For most of the locations in this study, the predominant P species was authigenic P, followed by Ex-P, Fe-P, OP and De-P. ZS-C was the only location that differed from this pattern, and even so, only authigenic and Ex-P were reversed (Fig. 2). In comparison with the locations in this study, only the northern Gulf of Mexico sediment core samples presented with authigenic P species as the largest fraction, representing 67–92% of TP, with the second highest P fraction being detrital P (5–21% of TP), and Fe-P, OP and Ex-P the three lowest [20]. Another location with the highest authigenic P was the central Pacific Ocean surface sediments, representing 43.4% TP, followed by detrital P (45.7%), OP, Fe-P and Ex-P [30]. Other locations such as East China Sea [33, 34, 46, 47], Sishili Bay [48] and the Caspian Sea [49] have De-P as the largest P fraction. Some studies have shown that the largest East China Sea P fraction is De-P, followed by OP, Fe-P and authigenic P [34, 46]; other studies have found that these sediments have more De-P, followed by authigenic P, OP and Fe-P [33] (Table 3).

In opposition to previous results on the Changjiang Estuary and East China Sea, our study areas showed that De-P was the lowest P fraction, indicating that these salt marshes and CE were receiving less riverine input. Our

results signify the importance of localized events on P cycling in salt marsh systems. The difference of P species in the CE in this study compared to those of previous studies could be attributable to different sampling times, as the riverine contribution to P in the CE at the time of our sampling may have been at its lowest. Moreover, the higher Ex-P in our study areas indicates that these sediments would be more prone to release P to the water column, even though these locations have an overall lower P contents.

5 Conclusion

The overall low TP and OP in the CE, AD and ZS salt marshes indicate that these locations were not polluted with P. Low De-P indicate that these locations did not receive much contribution from the riverine input. In fact, these locations were composed mostly of authigenic P, indicating contribution of apatite mineral probably from rock materials from their surrounding. The slightly higher authigenic P fraction in Zhoushan salt marshes A and B (60% of TP) compared to CE and Andong salt marsh (40% TP) indicates that the Zhoushan salt marshes were receiving input from the surrounding apatite minerals. Overall, these results indicate less P input from riverine discharge and more input from rock materials.

The slightly higher Fe-P in CE and Andong salt marshes compared to Zhoushan salt marshes could signify that CE and Andong salt marshes were likely to be oxic compared to the Zhoushan salt marshes. The overall high percentages of bioavailable P, which constituted of about 37–73% of the TP in these study areas, indicates that these locations may pose a threat by their potential contribution to eutrophication to their adjacent surrounding coastal zones. Higher Fe-P in CE and Andong salt marshes indicate that these P could be released to the water column during anoxic condition.

Acknowledgements We are grateful to Hong-Jiao Pang, Kang-Kang Yan and Xian-Hui Yang for help during samples collection. This work acknowledges the Zhejiang University Self Programme Fund for the Research of Heavy Metal Geochemical Characteristics in Sediments of Hangzhou Bay, Zhejiang University Fundamental Research Funds for the Central Universities 2013QNA4037, National Key Research and Development Plan of China (No. 2016YFC1401603) and National Natural Science Foundation of China (No. 41876031). The authors would like to thank the reviewers for constructive comments which have improved the manuscript.

Compliance with ethical standards

Conflict of interest There is no conflict of interest among the authors.

Appendix 1

See Table 4.

Table 4 Sampling time and locations' information

Location	Time	Depth	Longitude (N)	Latitude (E)
Changjiang Estuary				
20	23 August 2014	15.0 m	31.768°	121.103°
4	23 August 2014	13.7 m	31.276°	121.870°
6	23 August 2014	9.1 m	31.252°	121.994°
11	22 August 2014	23.6 m	31.106°	122.535°
13	22 August 2014	39.0 m	31.101°	122.805°
21	22 August 2014	57.0 m	31.101°	123.000°
Andong salt marsh Transect A				
A8	14 August 2014	0–5 cm*	30.366°	121.193°
A7	14 August 2014	0–5 cm*	30.369°	121.193°
A6	14 August 2014	0–5 cm*	30.371°	121.192°
A5	14 August 2014	0–5 cm*	30.373°	121.192°
A4	14 August 2014	0–5 cm*	30.376°	121.192°
A3	14 August 2014	0–5 cm*	30.378°	121.192°
A2	14 August 2014	0–5 cm*	30.379°	121.191°
A1	14 August 2014	0–5 cm*	30.381°	121.191°
Andong salt marsh Transect C				
C10	14 September 2014	0–5 cm*	30.366°	121.185°
C9	14 September 2014	0–5 cm*	30.367°	121.186°
C8	14 September 2014	0–5 cm*	30.370°	121.186°
C7	14 September 2014	0–5 cm*	30.371°	121.186°
C6	14 September 2014	0–5 cm*	30.372°	121.185°
C3	14 September 2014	0–5 cm*	30.377°	121.184°
C2	14 September 2014	0–5 cm*	30.379°	121.184°
C1	14 September 2014	0–5 cm*	30.381°	121.184°

* The depths for Andong salt marsh locations represent the depths of the surface sediments; the depths for the Changjiang Estuary represent water depth

Appendix 2

See Table 5.

Table 5 Sampling locations in the Zhoushan salt marshes A, B and C which were visited on 10 March 2018

Sampling locations	Longitude (N°)	Latitude (E°)
A1	29.9913	122.1718
A2	29.9908	122.1728
A3	29.9902	122.1738
A4	29.9894	122.1748
A5	29.9890	122.1754
B1	30.0194	122.3353
B2	30.0188	122.3342
B3	30.0183	122.3322
B4	30.0185	122.3298
C1	29.9793	122.1975
C2	29.9789	122.1992
C3	29.9783	122.2011
C4	29.9778	122.2031
C5	29.9765	122.2071

Appendix 3

See Table 6.

Table 6 The concentrations and percentages of sedimentary P species in Andong salt marsh, Changjiang Estuary and Zhoushan salt marshes

Loc	Ex-P (mg/kg)	Fe-P (mg/kg)	Authigenic P (mg/kg)	De-P (mg/kg)	OP (mg/kg)	IP (mg/kg)	BAP (mg/kg)	TP (mg/kg)	Percentage (%)						
									Ex-P	Fe-P	Authigenic P	De-P	OP	IP	BAP
Andong salt marsh Transect A (AD-A)															
A8	49.94	20.14	37.98	3.13	11.98	111.19	82.06	123.17	40.55	16.35	30.84	2.54	9.73	90.27	66.62
A7	42.87	32.00	70.57	3.56	10.47	149.00	85.34	159.47	26.88	20.07	44.25	2.23	6.57	93.43	53.51
A6	44.48	18.21	39.93	2.84	11.13	105.46	73.82	116.59	38.15	15.62	34.25	2.44	9.55	90.45	63.32
A5	42.41	19.09	52.75	2.08	9.32	116.33	70.82	125.65	33.75	15.19	41.98	1.66	7.42	92.58	56.36
A4	31.30	34.27	58.94	2.30	9.40	126.81	74.97	136.21	22.98	25.16	43.27	1.69	6.90	93.10	55.04
A3	29.21	12.46	42.53	2.47	4.63	86.67	46.30	91.30	31.99	13.65	46.58	2.71	5.07	94.93	50.71
A2	20.68	22.60	89.58	1.98	4.45	134.84	47.73	139.28	14.85	16.23	64.32	1.42	3.19	96.81	34.27
A1	29.22	40.13	47.15	2.67	8.21	119.17	77.56	127.38	22.94	31.50	37.02	2.10	6.45	93.55	60.89
Mean	36.26	24.86	54.93	2.63	8.70	118.68	69.83	127.38	29.01	19.22	42.81	2.10	6.86	93.14	55.09
SD	10.02	9.50	17.70	0.54	2.82	18.93	14.81	19.60	8.67	6.15	10.21	0.47	2.16	2.16	9.94
Andong salt marsh Transect C (AD-C)															
C10	42.63	21.53	79.53	2.09	8.85	145.78	73.01	154.63	27.75	13.92	51.43	1.35	5.72	94.28	47.22
C9	66.56	25.81	51.99	1.95	7.79	146.31	100.16	154.10	43.19	16.75	33.74	1.27	5.06	94.94	65.00
C8	62.38	33.24	52.90	2.20	9.00	150.72	104.62	159.72	39.06	20.81	33.12	1.38	5.63	94.37	65.50
C7	71.43	16.78	74.02	2.91	13.47	165.14	101.68	178.61	39.99	9.39	41.44	1.63	7.54	92.46	56.93
C6	56.67	22.94	45.23	3.54	11.45	128.38	91.06	139.83	40.53	16.41	32.35	2.53	8.19	91.81	65.12
C3	41.38	16.72	64.19	2.77	7.44	125.06	65.54	132.50	31.23	12.62	48.45	2.09	5.62	94.38	49.46
C2	42.84	50.60	91.54	3.43	8.58	188.41	102.02	196.99	21.75	25.69	46.47	1.74	4.36	95.64	51.79
C1	43.55	31.17	76.60	3.78	7.36	155.10	82.08	162.46	26.81	19.19	47.15	2.33	4.53	95.47	50.52
Mean	53.43	27.35	67.00	2.83	9.24	150.61	90.02	159.86	33.77	16.85	41.77	1.79	5.83	94.17	56.44
SD	12.30	11.15	16.07	0.71	2.15	20.17	14.87	20.52	7.92	5.09	7.72	0.48	1.37	1.37	7.76
Changjiang Estuary (CE)															
20	33.38	15.94	66.75	2.43	3.05	118.50	52.37	121.55	27.46	13.11	54.92	2.00	2.51	97.49	43.09
4	46.72	9.20	73.02	2.80	13.98	131.74	69.90	145.72	32.06	6.31	50.11	1.92	9.59	90.41	47.97
6	47.91	26.90	66.45	2.69	6.71	143.95	81.52	150.66	31.80	17.85	44.11	1.79	4.45	95.55	54.11
11	60.13	31.19	83.05	2.45	14.79	176.82	106.11	191.61	31.38	16.28	43.34	1.28	7.72	92.28	55.38
13	55.36	17.74	59.61	2.14	18.11	134.85	91.21	152.96	36.19	11.60	38.97	1.40	11.84	88.16	59.63
21	36.03	25.28	61.45	2.97	18.55	125.73	79.86	144.28	24.97	17.52	42.59	2.06	12.86	87.14	55.35
Mean	46.59	21.04	68.39	2.58	12.53	138.60	80.16	151.13	30.64	13.78	45.67	1.74	8.16	91.84	52.59
SD	10.47	8.15	8.58	0.30	6.30	20.59	18.30	22.77	3.92	4.42	5.79	0.33	4.09	4.09	5.98
Zhoushan salt marsh B (ZS-B)															
B1	78.04	13.39	157.13	2.37	5.55	250.93	96.98	256.48	30.43	5.22	61.26	0.92	2.16	97.84	37.81
B2	63.61	21.73	185.66	2.93	9.87	273.93	95.21	283.80	22.41	7.66	65.42	1.03	3.48	96.52	33.55
B3	94.29	15.22	163.71	2.73	9.73	275.95	119.24	285.68	33.01	5.33	57.31	0.96	3.41	96.59	41.74

Table 6 (continued)

Loc	Ex-P (mg/kg)	Fe-P (mg/kg)	Authigenic P (mg/kg)	De-P (mg/kg)	OP (mg/kg)	IP (mg/kg)	BAP (mg/kg)	TP (mg/kg)	Percentage (%)						
									Ex-P	Fe-P	Authigenic P	De-P	OP	IP	BAP
B4	86.31	19.27	196.17	4.27	1.00	306.02	106.58	307.02	28.11	6.28	63.89	1.39	0.33	99.67	34.71
Mean	80.56	17.40	175.67	3.08	6.54	276.71	104.50	283.25	28.49	6.12	61.97	1.08	2.34	97.66	36.95
SD	13.11	3.79	18.32	0.83	4.20	22.60	11.20	20.72	4.52	1.13	3.55	0.21	1.47	1.47	3.66
Zhoushan salt marsh A (ZS-A)															
A1	83.53	26.08	155.60	3.18	8.19	268.39	117.80	276.58	30.20	9.43	56.26	1.15	2.96	97.04	42.59
A2	98.55	5.36	167.11	2.38	16.00	273.40	119.91	289.40	34.05	1.85	57.74	0.82	5.53	94.47	41.43
A3	106.30	15.04	178.07	3.54	2.49	302.95	123.83	305.44	34.80	4.92	58.30	1.16	0.82	99.18	40.54
A4	82.05	8.42	175.13	2.91	1.86	268.51	92.33	270.37	30.35	3.11	64.77	1.08	0.69	99.31	34.15
A5	85.79	9.49	224.62	2.95	1.89	322.85	97.17	324.74	26.42	2.92	69.17	0.91	0.58	99.42	29.92
Mean	91.24	12.88	180.11	2.99	6.09	287.22	110.21	293.31	31.16	4.45	61.25	1.02	2.12	97.88	37.73
SD	10.65	8.17	26.36	0.42	6.15	24.56	14.38	22.12	3.38	3.00	5.50	0.15	2.15	2.15	5.46
Zhoushan salt marsh C (ZS-C)															
C1	63.31	21.73	65.07	4.51	2.17	154.62	87.21	156.79	40.38	13.86	41.50	2.88	1.38	98.62	55.62
C2	72.85	16.78	28.77	2.93	2.45	121.33	92.08	123.78	58.85	13.56	23.24	2.37	1.98	98.02	74.39
C3	116.09	9.50	16.90	2.38	2.15	144.87	127.74	147.02	78.96	6.46	11.50	1.62	1.46	98.54	86.89
C4	99.50	15.06	42.74	5.04	10.24	162.34	124.80	172.58	57.65	8.73	24.77	2.92	5.93	94.07	72.31
C5	90.78	32.46	36.07	4.54	5.95	163.85	129.19	169.80	53.46	19.12	21.24	2.67	3.50	96.50	76.08
Mean	88.51	19.11	37.91	3.88	4.59	149.40	112.20	153.99	57.86	12.34	24.45	2.49	2.85	97.15	73.06
SD	21.02	8.65	17.95	1.15	3.54	17.41	20.73	19.78	13.89	4.93	10.84	0.53	1.92	1.92	11.26

Ex-P = exchangeable P; Fe-P = iron-bound P; De-P = detrital P; OP = organic P; IP = inorganic P; BAP = bioavailable P; TP = total P; P = phosphorus; IP = Ex-P + Fe-P + authigenic P + De-P; OP + IP = TP; BAP = Ex-P + Fe-P + OP

Appendix 4

See Table 7.

Table 7 Proportions of sedimentary P species for each system

Locations	Concentration of P species (mg/kg)
(a) Mg/kg	
AD	authigenic P (37.98–91.54 mg/kg) > Ex-P (20.68–71.43 mg/kg) > Fe-P (12.46–50.60 mg/kg) > OP (4.45–13.47 mg/kg) > De-P (1.95–3.78 mg/kg)
CE	authigenic P (59.61–83.05 mg/kg) > Ex-P (33.38–60.13 mg/kg) > Fe-P (9.20–31.19 mg/kg) > OP (3.05–18.55 mg/kg) > De-P (2.14–2.97 mg/kg)
ZS-A and Ad-B	authigenic P (155.60–224.62 mg/kg) > Ex-P (63.61–106.30 mg/kg) > Fe-P (5.36–26.08 mg/kg) > OP (1–16 mg/kg) > De-P (2.37–4.27 mg/kg)
ZS-C	Ex-P (63.31–116.09 mg/kg) > authigenic P (16.90–65.07 mg/kg) > Fe-P (9.50–32.46 mg/kg) > OP (2.15–19.24 mg/kg) > De-P (2.38–5.04 mg/kg)
Locations	Percentages of P species
(b) Percentages	
AD-A	Authigenic P (42.81%) > Ex-P (29.01%) > Fe-P (19.22%) > OP (6.86%) > De-P (2.10%)
AD-C	Authigenic P (41.77%) > Ex-P (33.77%) > Fe-P (16.85%) > OP (5.83%) > De-P (1.79%)
CE	Authigenic P (45.67%) > Ex-P (30.64%) > Fe-P (13.78%) > OP (8.16%) > De-P (1.74%)
ZS-A	Authigenic P (61.25%) > Ex-P (31.16%) > Fe-P (4.45%) > OP (2.12%) > De-P (1.02%)
ZS-B	Authigenic P (61.97%) > Ex-P (28.49%) > Fe-P (6.12%) > OP (2.34%) > De-P (1.08%)
ZS-C	Ex-P (57.86%) > Authigenic P (24.45%) > Fe-P (12.34%) > OP (2.85%) > De-P (2.49%)

Appendix 5

See Table 8.

Table 8 Correlations results among the P species

	Ex-P	Fe-P	Authigenic P	De-P	OP	IP	TP
(a) Andong salt marsh Transect A (AD-A)							
Ex-P	1.00						
Fe-P	−0.21	1.00					
Authigenic P	−0.55	0.25	1.00				
De-P	0.63	0.20	−0.27	1.00			
OP	0.89*	0.20	−0.48	0.62	1.00		
IP	−0.07	0.63	0.76*	0.21	0.17	1.00	
TP	0.06	0.64	0.67	0.29	0.31	0.99*	1.00
(b) Andong salt marsh Transect C (AD-C)							
Ex-P	1.00						
Fe-P	−0.28	1.00					
Authigenic P	−0.52	0.42	1.00				
De-P	−0.34	0.30	0.28	1.00			
OP	0.61	−0.33	−0.11	0.14	1.00		
IP	0.03	0.73*	0.72*	0.21	0.11	1.00	
TP	0.09	0.68	0.70	0.22	0.21	0.99*	1.000
(c) Changjiang Estuary							
Ex-P	1.00						
Fe-P	0.32	1.00					
Authigenic P	0.48	0.26	1.00				
De-P	−0.49	0.05	0.03	1.00			
OP	0.40	0.11	−0.09	0.07	1.00		
IP	0.83*	0.67	0.76*	−0.20	0.21	1.00	
TP	0.86*	0.63	0.66	−0.16	0.47	0.96*	1.00
(d) Zhoushan salt marsh A (ZS-A)							
Ex-P	1						
Fe-P	−0.19	1					
Authigenic P	−0.12	−0.42	1				
De-P	0.19	0.63	0.01	1			
Or-P	0.24	−0.11	−0.52	−0.68	1		
TP	0.34	−0.23	0.84*	0.17	−0.28	1	
(e) Zhoushan salt marsh (ZS-B)							
Ex-P	1						
Fe-P	−0.55	1					
Authigenic P	−0.23	0.87*	1				
De-P	0.20	0.55	0.88*	1			
Or-P	−0.25	0.02	−0.43	−0.72	1		
TP	0.28	0.63	0.84*	0.90*	−0.37	1	
(f) Zhoushan salt marsh C (ZS-C)							
Ex-P	1						
Fe-P	−0.42	1					
Authigenic P	−0.71	0.40	1				
De-P	−0.29	0.56	0.75*	1			
Or-P	0.31	0.14	0.12	0.71	1		
TP	0.27	0.41	0.39	0.80*	0.72	1	

*Indicates *p* is significant to 0.05

References

1. Roner M, D'Alpaos A, Ghinassi M, Marani M, Silvestri S, Franceschinis E, Realdon N (2016) Spatial variation of salt-marsh organic and inorganic deposition and organic carbon accumulation: inferences from the Venice lagoon, Italy. Adv Water Resour 93:276–287
2. Gonneea ME, Maio CV, Kroeger KD, Hawkes AD, Mora J, Sullivan R, Madsen S, Buzard RM, Cahill N, Donnelly JP (2019) Salt marsh ecosystem reconstructing enhances elevation resilience and carbon storage during accelerating relative sea-level rise. Estuar Coast Shelf Sci 217:56–68
3. Jiménez-Cárceles FJ, Álvarez-Rogel J (2008) Phosphorus fractions and distribution in salt marsh soils affected by mine wastes and eutrophicated water: a case study in SE Spain. Geoderma 144:299–309
4. González-Alcaraz MN, Egea C, Jimenez-Carceles FJ, Parraga I, Maria-Cervantes A (2012) Storage of organic carbon, nitrogen and phosphorus in the soil-plant system of phragmites australis stands from a eutrophicated Mediterranean salt marsh. Geoderma 185–186:61–72
5. Bonometto A, Feola A, Rampazzo F, Gion C, Berto D, Ponis E, Boscolo Brusà R (2019) Factors controlling sediment and nutrient fluxes in a small microtidal salt marsh within the Venice Lagoon. Sci Total Environ 650:1832–1845
6. Crosby SC, Sax DF, Palmer ME, Booth HS, Deegan LA, Bertness MD, Leslie HM (2016) Salt marsh persistence is threatened by predicted sea-level rise. Estuar Coast Shelf Sci 181:93–99
7. Valiela I, Lloret J, Bowyer T, Miner S, Remsen D, Elmstrom E, Cogswell C, Thieler ER (2018) Transient coastal landscapes: rising sea level threatens salt marshes. Sci Total Environ 640–641:1148–1156
8. Velinsky DJ, Paudel B, Belton TJ, Sommerfield CK (2017) Tidal marsh record of nutrient loadings in Barnegat Bay, New Jersey. J Coast Res 78:79–88
9. Yang W, Li N, Leng X, Qiao Y, Cheng X, An S (2016) The impact of sea embankment reclamation on soil organic carbon and nitrogen pools in invasive Spartina alterniflora and native Suaeda salsa salt marshes in eastern China. Ecol Eng 97:582–592
10. Huang L, Bai J, Chen B, Zhang K, Huang C, Liu P (2012) Two-decade wetland cultivation and its effects on soil properties in salt marshes in the Yellow River Delta, China. Ecol Inform 10:49–55
11. Wasson K, Jeppesen R, Endris C, Perry DC, Woolfolk A, Beheshti K, Rodriguez M, Eby R, Watson EB, Rahman F, Haskins J, Hughes BB (2017) Eutrophication decreases salt marsh resilience through proliferation of algal mats. Biol Conserv 212:1–11
12. Tatariw C, Floarnoy N, Kleihuizen AA, Tollette D, Overto EB, Sobecky PA, Mortazavi B (2018) Salt marsh denitrification is impacted by oiling intensity six years after the Deepwater Horizon oil spill. Environ Pollut 243:1606–1614
13. Mudd SM, Howell SM, Morris JT (2009) Impact of dynamic feedbacks between sedimentation, sea-level rise, and biomass production on near-surface marsh stratigraphy and carbon accumulation. Estuar Coast Shelf Sci 82:377–389
14. Dafner EV, Mallin MA, Souza JJ, Wells HA, Parsons DC (2007) Nitrogen and phosphorus species in coastal and shelf waters of Southeastern North Carolina, Mid-Atlantic U.S. coast. Mar Chem 103:289–303
15. Gao Z, Bai J, Jia J, Wen X, Zhang G, Zhao Q (2015) Spatial and temporal changes of phosphorus in coastal wetland soils as affected by a tidal creek in the Yellow River Estuary, China. Phys Chem Earth 89–90:114–120
16. Alvarez-Rogel J, Jimenez-Carceles FJ, Egea-Nicolas C (2007) Phosphorus retention in a coastal salt marsh in SE Spain. Sci Total Environ 378:71–74
17. Guinard MS, Leitch AR, Acquisti C, Eizaguire C, Elser JJ, Hessen DO, Jeyasingh PD, Neiman M, Richardson AE, Soltis PS, Soltis DE, Stevens CJ, Trimmer M, Weider LJ, Woodward G, Leitch IJ (2017) Impacts of nitrogen and phosphorus: from genomes to natural ecosystems and agriculture. Front Ecol Evol 5:70
18. Jansson M, Enell M, Fleischer S, Gächter R, Keldermann P, Löfgren S, Nürnberg G, Provini A, Sinke A (1988) Phosphorus release from lake sediments. Arch Hydrobiol Beih Ergebn Limnol 30:90–93
19. SØndergaard M, Jensen JP, Jeppesen E (2003) Role of sediment and internal loading of phosphorus in shallow lakes. Hydrobiology 506–509:135–145
20. Adhikari PL, White JR, Maiti K, Nguyen N (2015) Phosphorus speciation and sedimentary phosphorus release from the Gulf of Mexico sediments: implication for hypoxia. Estuar Coast Shelf Sci 164:77–85
21. Nürnberg GK (1988) Prediction of phosphorus release rates from total and reductant-soluble phosphorus in anoxic lake sediments. Can J Fish Aquat Sci 45:453–462
22. Hiriart-Baer VP, Milne JE, Marvin CH (2011) Temporal trends in phosphorus and lacustrine productivity in Lake Simcoe inferred from lake sediment. J Great Lakes Res 37:764–771
23. Kopáček J, Borovec J, Hejzlar J, Ulrich K-U, Norton SA, Amirbahman A (2005) Aluminum control of phosphorus sorption by lake sediments. Environ Sci Technol 39:8784–8789
24. Yang B, Liu S-M, Wu Y, Zhang J (2016) Phosphorus speciation and availability in sediments off the eastern coast of Hainan Island, South China Sea. Cont Shelf Res 118:111–127
25. Loh PS, Molot LA, Nürnberg GK, Watson SB, Ginn B (2013) Evaluating relationships between sediment chemistry and anoxic phosphorus and iron release across three different water bodies. Inland Waters 3:105–118
26. Zhang Y, Du J, Zhao X, Wu W, Peng B, Zhang J (2014) A multiproxy study of sedimentary humic substances in the salt marsh of the Changjiang Estuary, China. Estuar Coast Shelf Sci 151:295–301
27. Shan B, Li J, Zhang W, Di Z, Jin X (2016) Characteristics of phosphorus components in the sediments of main rivers into the Bohai Sea. Ecol Eng 97:426–433
28. Łukawska-Matuszewska K, Kiełczewska J, Bolałek J (2014) Factors controlling spatial distributions and relationships of carbon, nitrogen, phosphorus and sulphur in sediments of the stratified and eutrophic Gulf of Gdansk. Cont Shelf Res 85:168–180
29. Kraal P, Bostick BC, Behrends T, Reichart G-J, Slomp CP (2015) Characterization of phosphorus species in sediments from the Arabian Sea oxygen minimum zone: combining sequential extractions and X-ray spectroscopy. Mar Chem 168:1–8
30. Ni J, Lin P, Zhen Y, Yao X, Guo L (2015) Distribution, source and chemical speciation of phosphorus in surface sediments of the central Pacific Ocean. Deep-Sea Res I 105:74–82
31. Kraal P, Dijkstra N, Behrends T, Slomp CP (2017) Phosphorus burial in sediments of the sulfidic deep Black Sea: key roles for adsorption by calcium carbonate and apatite authigenesis. Geochim Cosmochim Acta 204:140–158
32. Lu D, Guo P, Ji J, Liu L, Yang P (2016) Evaluation of phosphorus distribution and bioavailability in sediments of a subtropical wetland reserve in southeast China. Ecol Indic 66:556–563
33. Zhou F, Gao X, Yuan H, Song J, Chen C-TA, Lui H-K, Zhang Y (2016) Geochemical forms and seasonal variations of phosphorus in surface sediments of the East China Sea shelf. J Mar Syst 159:41–54

34. Yang B, Song G-D, Liu S-M, Jin J (2017) Phosphorus recycling and burial in core sediments of the East China Sea. Mar Chem 192:59–72
35. Cao W, Li R, Chi X, Chen N, Chen J, Zhang H, Zhang F (2017) Island urbanization and its ecological consequences: a case study in the Zhoushan Island, East China. Ecol Indic 76:1–14
36. Kang XM, Song JM, Yuan HM, Shi X, Yang WF, Li XG, Li N, Duan LQ (2017) Phosphorus speciation and its bioavailability in sediments of the Jiaozhou Bay. Estuar Coast Shelf Sci 188:127–136
37. Zhang WL, Zeng CS, Tong C, Zhai SJ, Lin X (2015) Spatial distribution of phosphorus speciation in marsh sediments along a hydrologic gradient in a subtropical estuarine wetland, China. Estuar Coast Shelf Sci 154(154):30–38
38. Che Y, He Q, Lin WQ (2003) The distributions of particulate heavy metals and its indication to the transfer of sediments in the Changjiang Estuary and Hangzhou Bay, China. Mar Pollut Bull 46:123–131
39. Xie DF, Gao S, Wang ZB, Pan CH (2013) Numerical modeling of tidal currents, sediment transport and morphological evolution in Hangzhou Bay, China. Int J Sediment Res 28:316–328
40. Yuan HW, Chen JF, Ye Y, Lou ZH, Jin AM, Chen XG, Jiang ZP, Lin Y-S, Chen C-TA, Loh PS (2017) Sources and distribution of sedimentary organic matter along the Andong salt marsh, Hangzhou Bay. J Mar Syst 174:78–88
41. Pan Y, Zhai M, Lin L, Lin Y, Cai J, Deng J-S, Wang K (2016) Characterizing the spatiotemporal evolutions and impact of rapid urbanization on island sustainable development. Habitat Int 53:215–227
42. Xu G, Liu J, Liu S, Wang Z, Hu G, Kong X (2016) Modern muddy deposit along the Zhejiang coast in the East China Sea: response to large-scale human projects. Conti Shelf Res 130:68–78
43. Ruttenberg KC (1992) Development of a sequential extraction method for different forms of phosphorus in marine sediments. Limnol Oceanogr 37(7):1460–1482
44. Andrieux-Loyer F, Aminot A (2001) Phosphorus forms related to sediment grain size and geochemical characteristics in French coastal areas. Estuar Coast Shelf Sci 52:617–629
45. Kaiserli A, Voutsa D, Samara C (2002) Phosphorus fractionation in lake sediments—Lakes Volvi and Koronia, N. Greece. Chemosphere 46:147–1155
46. Meng J, Yao P, Yu Z, Bianchi TS, Zhao B, Pan H, Li D (2014) Speciation, bioavailability and preservation of phosphorus in surface sediments of the Changjiang Estuary and adjacent East China Sea inner shelf. Estuar Coast Shelf Sci 144:27–38
47. Zheng L, Ye Y, Zhou H (2004) Phosphorus forms in sediments of the East China and its environmental significance. J Geogr Sci 14(1):113–120
48. Zhang Y, Gao X, Wang C, Chen C-TA, Zhou F, Yang Y (2016) Geochemistry of phosphorus in sediment cores from Sishili Bay, China. Mar Pollut Bull 113:552–558
49. Bastami KD, Neyestani MR, Raeisi H, Shafeian E, Baniamam M, Shirzadi A, Esmaeilzadeh M, Mozaffari S, Shahrokhi B (2018) Bioavailability and geochemical speciation of phosphorus in surface sediments of the Southern Caspian Sea. Mar Pollut Bull 126:51–57